Effect of iron doping on $PbTiO_3$ perovskites to enhance material properties for technological applications

M. Safdar [a], A. D. Khalid [b,*], M. Sharif [c], S. Akbar [d], M. I. Khan [e], M. Yosif [f], M. S. Hasan [g], S. M. El-Bahy [h], M. N. Khan [i], A. Almohammedi [i]

[a] *Centre of Excellence in Solid State Physics, University of the Punjab Lahore, Pakistan*

[b] *University Institute of Radiological Sciences and Medical Imaging Technology, The University of Lahore, Lahore, Pakistan*

[c] *Department of DNA and Serology Punjab Forensic Science Agency, Lahore Pakistan*

[d] *College of pharmacy, University of Sargodha, Sargodha, Pakistan*

[e] *Department of Physics, the University of Lahore, Lahore Pakistan*

[f] *Institute of Physics, The Islamia university of Bahawalpur, Pakistan*

[g] *Institute of Functional Nano &SoftMaterials (FUNSOM), Jiangsu KeyLaboratory for Carbon-Based FunctionalMaterials& Devices, Soochow University,Suzhou, China*

[h] *Department of Chemistry, Turabah University College, Taif University, P.O. Box 11099, Taif 21944, Saudi Arabia*

[i] *Department of Physics, Faculty of Science, Islamic University of Madinah, Madinah, 42351, Saudi Arabia*

Iron-doped titanate ($PbTi_{1-x}Fe_xO_3$) was successfully synthesized using the sol-gel auto-combustion method, with varying iron concentrations (x = 0.00, 0.02, 0.04, 0.06, 0.08, and 0.1). Elemental composition was determined by EDS, morphology was analyzed using SEM, and ferroelectric properties were evaluated through the P-E loop and PUND methods. EDS confirmed the successful incorporation of Fe into the structure. SEM images showed a reduction in the particle size of $PbTiO_3$, from 100 nm to 20 nm, suggesting that the presence of Fe ions contributed to the decrease in particle size. Ferroelectric analysis indicated a reduction in polarization, enhanced coercivity, and minimal leakage current at an iron concentration of x = 0.02, making it suitable for energy storage applications.

(Received January 22, 2025; Accepted July 14, 2025)

Keywords: Titanate, doping, ferroelectric, polarization, coercivity

1. Introduction

The magneto-electric multiferroic related to the magnetic and ferroelectric demands have focused great devotion for potential uses [1-4]. The multiferroics and ferroelectric materials are focused largely but are most focuses is active micro electronics devices and components [5-6]. The materials which are based on ferroelectric $XTiO_3$ (X= Pb, Sr, Ba etc) with properties of high permittivity, ferroelectric at room temperature, extraordinary polarization and considerable piezoelectric are extremely used in electronics such as multilayer capacitors, resonators, memory devices and resonators etc. [7-8]. In past decades these materials have focused great interest as are technical and are research relevant [9-11]. The ferroelectric perovskite is extremely focused as it is one of the vital materials systems for multiferric investigation, with tunable magnetic and electric order, after the discovery of trends of perovskites including $BiFeO_3$ and $TbMnO_3$ [12-13]. In past decade many multiferric materials have been proposed due to their different physical origins [14]. The magneto electric linked effect expected among the ferroelectric materials having magnetic

* Corresponding author: ad_khalid82@hotmail.com
https://doi.org/10.15251/DJNB.2025.203.781

structure that can induce spin induced multi ferric materials [15]. In the last decades, the $PbTiO_3$ focused more in different electronics application such as in electronic devices, sensors, phase shifters and tunable filters [16]. The $PbTiO_3$ have stable perovskite phase so is most promising material because of its mophotropic phase boundary [17]. The controllable ferroelectric materials can be applying in many nano scale ferroelectric devices such as electro optic, solar and energy garnering devices and dense memory devices [18-20]. The perovskite also focused more attention polarization [21]. The most recent applications of multi ferric lead TiO_3 – based perovskites are in digital computer memories with low high speed and low power consumption [22]. Therefore multiferroic Pb base perovskites are being synthesized by substituting magnetic citations such as $Pb(Fe_{2/3}\ W_{1/3})O_3$ [23] $Pb(Fe_{1/2}\ Ta_{1/2})$ [24] $Pb(Fe\ Ta)O_3$ [25] and $PbTi\ PdO_3$[26] which changes the properties by replacing the diamagnetic Ti^{4+} . The many multiferroic have been fabricated by introducing Ti^{4+} site into $PbTiO_3$ [27]. Hasitha Ganegoda and Soham Mukherjee et al. investigated the effect of Fe doing on local structure and magnetic properties of $PbTiO_3$ nanostructure, they concluded their magnetic properties enhanced by doping of Fe and exist as ferroelectric and magnetic phases [28]. Zahir Muhammad and M.U.U. Ishafaq et al. studied the influence of Ni doing on electrical and magnetic properties of $PbTiO_3$ nanostructure; they concluded their magnetic properties enhanced by doping of Ni and occur as multiferroic properties [29]. Y Sakout, and O.I Ghadraoui et al. enhanced the dielectric properties of $PbTiO_3$ nanoparticles by Ni doping [30]. Amrita Nayak and S.K. Patri at al reported their review article that the electric and magnetic properties of PbTiO3 perovskite were enhanced by Fe doping [31]. In the present we synthesize Fe-doped lead titanate ($PbTi_{1-x}\ Fe_xO_3$) with different concentration of Fe (x=0.00, 0.02, 0.04, 0.06, 0.08 and 0.1) by sol gel auto combustion route and investigated their morphological and magnetic properties by changing the doping concentration. Sol-gel is most famous, low cost, low temperature and easy to handle method as compared to other methods [32]. The SEM images disclose shrinkage of particle size with growing doping concentration this decrease in particle size could be advantages in specific uses. The ferroelectric study was achieved by P-E loops which reflects the increasing polarization and with highest doing concentration of Fe. Further more moderate iron doing (x=0.02) delivers best performance of ferroelectric performance which is useful in energy storage devices and electronics uses.

2. Materials and method

The lead titanate ($PbTi_{1-x}\ Fe_xO_3$) iron doped at different concentration (x= 0.00, 0.02, 0.04, 0.06, 0.08 and 1.0) was synthesized by sol-gel auto combustion route. The precursors used were Lead acetate ($Pb(C_2H_3O_2)_2$), Titanium dioxide (TiO_2), Iron oxide (Fe_2O_3),Iron nitrate ($Fe(NO_3)_3$), acetone, ethanol and distilled water. For synthesis, initially lead acetate, titanium dioxide and iron oxide were weighted according to required concentration then raw were mixed in a stoichiometric ratio by mill which uniformly distributes Fe^{3+} ions in the TiO_2 lattice. The mixture dissolved in distilled water to prepare homogeneous solution. Then mixture was calcinated at 800 ^{0}C in the furnace for 6 hours to get perovkite structure. After calcination, the powder was again grinded to avoid any agglomerates. Finally, the pellets were sintered at temperature of 1100 ^{0}C for 4 hours to get crystalline structure and then were cooled at room temperature.

2.1. Characterization techniques

The synthesized samples were analyzed using various techniques, including EDS to determine the elemental composition, SEM to examine the sample morphology, and the ferroelectric properties were studied using the P-E loop and PUND methods.

3. Results and discussion

3.1. EDS analysis

The elemental composition of all the samples was determined using EDS to predict the effects of doping. The EDS analysis of the pure PTO sample is shown in Figure 1. The analysis reveals a prominent peak for Pb, accounting for approximately 58%, while Ti makes up 11% and O constitutes 16%. These findings confirm the dominant presence of Pb, with intermediate peaks for Ti and O, indicating the successful formation of the sample. The EDS data for doped PTO (x = 0.02) is presented in Figure 1. The results clearly show that the sharpest peak corresponds to approximately 62 weight percent, representing 62% Pb. There are also smaller peaks with weight percentages of 13% for Ti and 15% for O, as indicated by the EDS analysis, confirming that Pb is the dominant element, while Ti and O show intermediate peaks. No peak for Fe is observed due to its low doping concentration, resulting in minimal intensity. The EDS results for doped PTO (x = 0.04) are presented in Figure 1. The analysis shows approximately 55% Pb, 12% Ti, and 14% O, based on the EDS data of the sample. This confirms a prominent peak for Pb, with intermediate peaks for Ti and O. No peak for Fe is detected, likely due to the low concentration of doping. With an increase in doping, specifically at x = 0.06, a peak corresponding to Fe appears with a weight of approximately 7%. This is attributed to the higher intensity of reflected beams from Fe. Meanwhile, the weight percentage of Ti decreases by about 9%, indicating the successful substitution of Ti by Fe. Additionally, the sample contains around 17% oxygen and 55% lead, as illustrated in Figure 1.With an additional increase, specifically for x = 0.08, Fe is found to be around 14%, while Ti decreases to about 7%, as shown in Figure 1. At this point, the sample exhibits a dominant peak for Pb, with a weight percentage of approximately 48%. In the final sample (x = 0.1), Fe constitutes approximately 20%, while Ti decreases to around 4%. O makes up about 23%, and Pb accounts for 45% of the total weight, as shown in Figure 1. The decrease in Ti and the increase in Fe confirm that the concentration of Fe rises in each subsequent sample due to the increase in Fe doping.

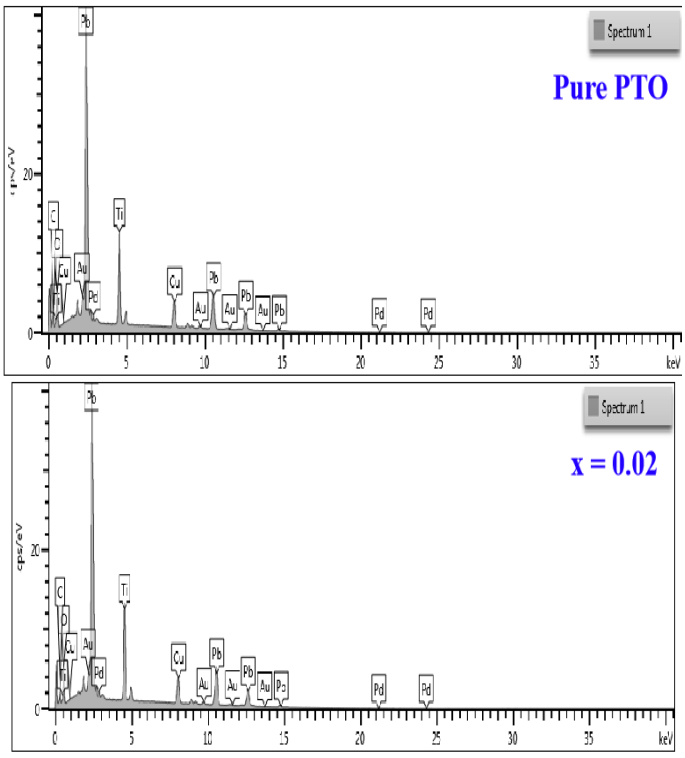

Figure 1.a) EDS images for pure PTO and x = 0.02, 0.04, 0.06, 0.08 and 0.1 concentrations.

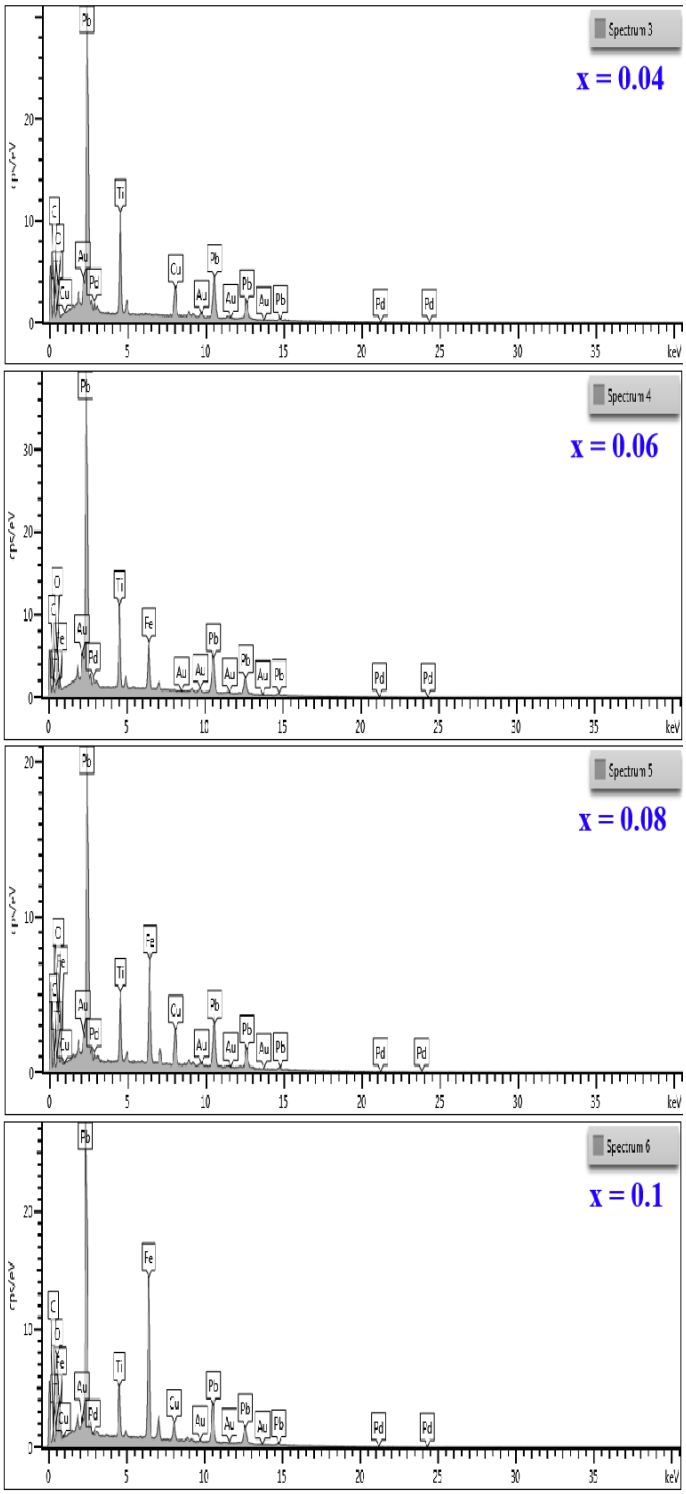

Figure 1.b) EDS images for pure PTO and x = 0.02, 0.04, 0.06, 0.08 and 0.1 concentrations.

3.2. SEM analysis

The surface morphology was examined by Scanning Electron Microscopy (SEM). The pure PTO and doped with iron in different concentration changes in the morphology with the increment of dopant as x = 0.00, 0.02, 0.04, 0.06, 0.08 and 0.1 in $PbTi_{1-x}Fe_xO_3$. Figure 2 shows SEM images for pure sample for x = 0.00 i.e. pure PTO. It can be seen clearly that average particle size is about 100 nm. There is agglomeration of particles having a bit granular nature. This

agglomeration may due the magnetic nature of the sample. A good thing is that there is almost continuous nature of agglomeration which helps us in using the sample for different applications. For x = 0.02, Figure 2 shows SEM images for the doped sample at different resolutions. It can be seen clearly that average particle size reduces up to 70 nm. There is less agglomeration of particles than the pure sample. Shape of the sample is different as it has mostly particles in the shape of squares boxes. For x = 0.04, Figure 2 shows SEM images for as doped sample at different resolutions. It can be seen that average particle size is about 50 nm. There is less agglomeration of particles with reduction in their size due to increment of dopant. For x = 0.06, Figure 2 shows SEM images for the doped sample at different resolutions. It can be seen clearly that average particle size reduces up to 25 nm. There is less agglomeration of particles than the previous sample. For x = 0.08, Figure 2 shows SEM images for as doped sample at different resolutions. It can be seen clearly that average particle size reduces up to 25 nm. The sample is like sand and mud particles with having rocks of different sizes on their surface. Most of the particles have similar shapes. The trend continues and particle size reaches 20 nm which means pure PFO sample has comparatively less particle size along with agglomeration as compared to doped and pure PTO as shown in Figure 2. We have concluded that the particles size of host material decreases by increasing doping concentration it may be due to trapping effect which is produced by grain boundaries and Fe ions furthermore the dragging force between Fe ions and grain boundaries and Fe also reduces the particle size [33]. The reduction particles size was also reported when Fe was doped in BCT Perovskites [34]. The doping of Fe in (Ba-Ca) TiO_3 also reduced the particle size [35]. The same result was also reported by Amrita Nayak in his review article [36].

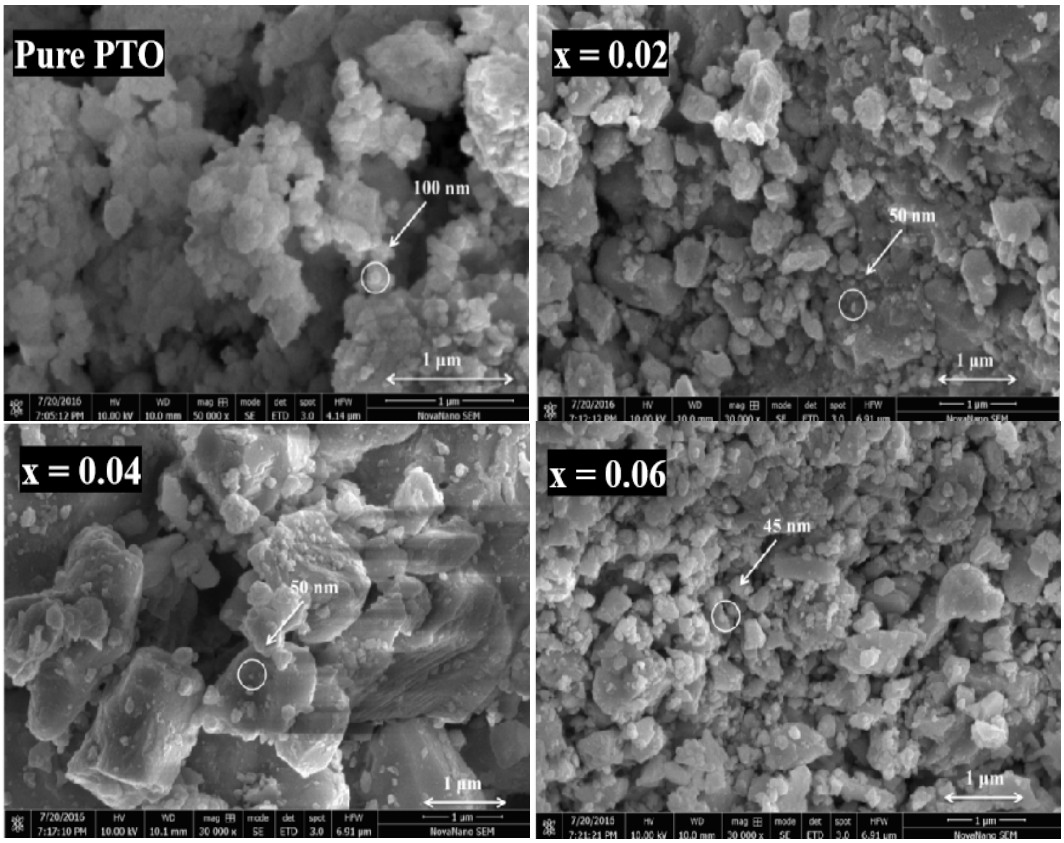

Figure 2.a) SEM images for pure PTO and x = 0.02, 0.04, 0.06, 0.08 and 0.1 concentrations.

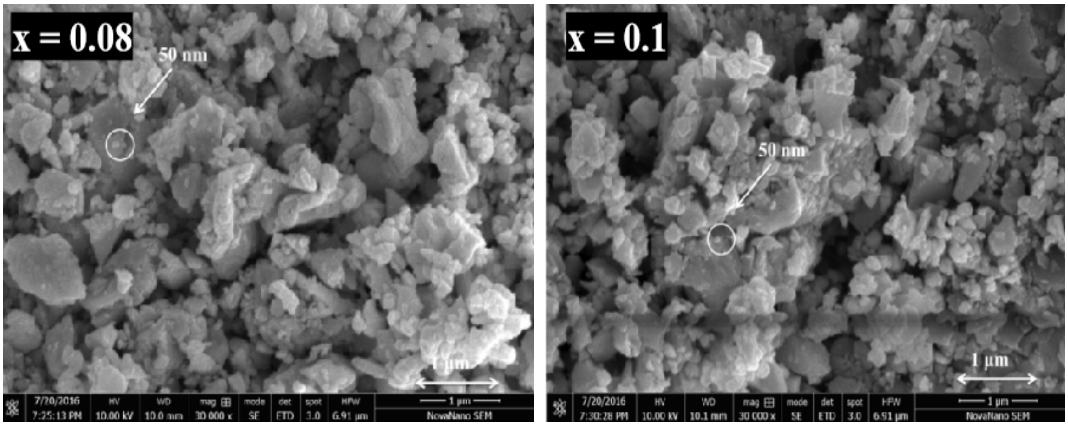

Figure 2.b. SEM images for pure PTO and x = 0.02, 0.04, 0.06, 0.08 and 0.1 concentrations.

3.3. Ferroelectric analysis

The ferroelectric behavior of pure sample and Fe doping at different concentration has been investigated by recording polarization and applied electric field (P-E) hysteresis loop at frequency of 50 Hz varying with doping and electric field. The behavior of ferroelectric properties strongly depends on different factors such as temperature, axial ratio, grain size, ionic radius and phase transition [37, 38]. The variation of polarization verses electric field was recorded at room temperature for $PbTi_{1-x}Fe_xO$ with varying iron concentrations (x = 0.00, 0.02, 0.04, 0.06, 0.08, and 0.10) and at different applied electric field (100-600KV) are represented in figure3 (a-d). For each doped composition is denoted by figure 3(a), it can be seen that loop becomes more saturated and shriller at x=0.02, and then thickness increases by increasing doping intensity. The variation of polarization verses applied electric field was investigating and shown in figure 3 (c), which reflects that the polarization decreases with intensity of applied field the this may be recognized the improvement of ferroelectric domains with increasing applied electric field [39].The Figure 3 (b) reflects that the value of maximum polarization (P_m) for the pure PTO is found to be 0.46485 nC/cm^2 and similarly remanence (P_r) is about 0.33208 nC/cm^2. It can be seen from the P-E curve that these values go on decreasing with increase in doping concentration and for x = 0.08 these are found to be 0.35067 nC/cm^2 and 0.29006 nC/cm^2. Corecivity (E_c) of all the samples shows the trend from minimum (for x = 0.0) 58.196 kV/cm to maximum (for x=0.08) 68.912 kV/cm. for x= 0.10 i.e. for pure PTO sample maximum polarization (P_m) is about 0.2871 nC/cm^2, and remanence (P_r) is about 0.1434 nC/cm^2 and it has coericivity value of about 42 kV/cm. All these values are obtained by applying electric potential in the range of 100kV/cm to 600kV/cm.

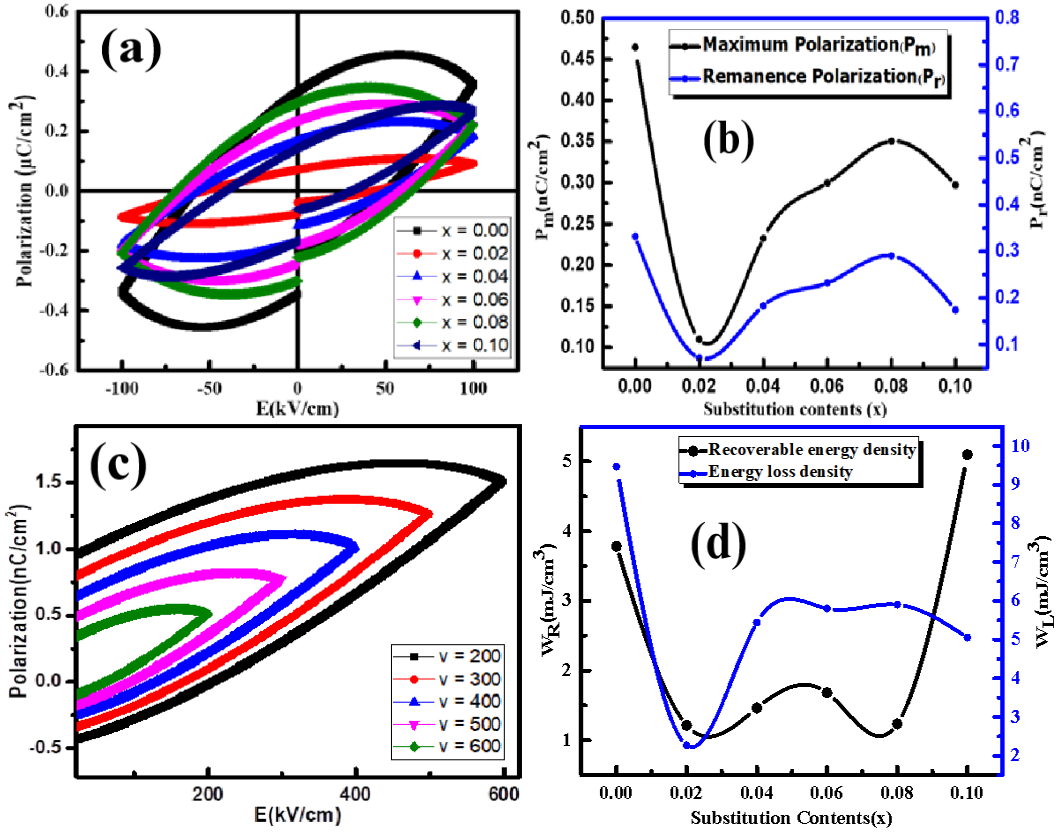

Figure 3. (a) Polarization vs substitution content(x), b) Maximum Polarization (P_m) and Remnance Polarization (P_r) vs. substitution content(x),c) Polarization vs. Electric Field loops and d) Variation of Recoverable Energy Density (W_R) and Energy Loss Density (W_L).

It is confirmation from hysteresis loop that all the samples have typical ferromagnetic properties. It also proved that intensity of polarization and loop density is highly affected by Fe content. The values of P_m and P_r and Ec obtained from all samples are listed in Table 1 Review the data presented in Table 1, it has been perceived that by increasing doping intensity of Fe leads to decrease in P_r and Ec. This may due to disturbance in polarization between grains because of increasing number of grain boundaries which leads to decreasing the grain size (observed in SEM images) with increasing Fe concentration [40]. The figure 3 (d) it shows that the energy loss density depends on doping concentration which is minimum at x=0.02.

Table 1. Values of P_m ,P_r and E_c for x = 0.00, 0.02, 0.04, 0.06, 0.08 and 0.1.

X	*P_m(nC/cm²)*	*P_r(nC/cm²)*	*E_c(kV/cm)*
0.00	0.46485	0.33208	58.196
0.02	0.10976	0.71477	53.864
0.04	0.23242	0.18315	57.227
0.06	0.29968	0.23234	63.554
0.08	0.35067	0.29006	68.912
0.1	0.2871	0.1434	41.72

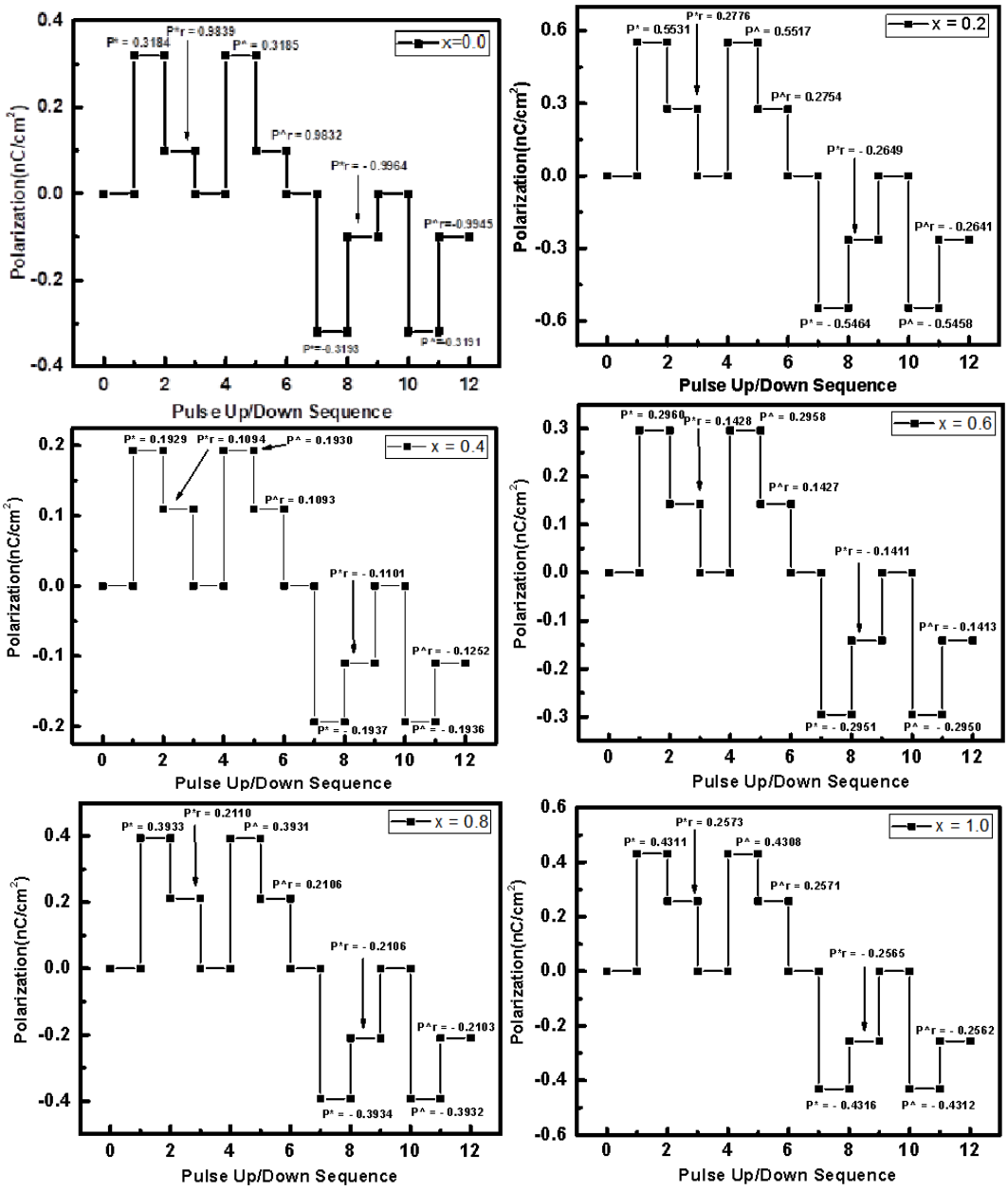

Figure 4. PUND sequence for x = 0.0, 0.02, 0.04, 0.06, 0.08 and 0.1 and switching energy density vs. substitution content.

Figure 4 shows the ferroelectric properties of $PbTi_{1-x}Fe_xO_3$at (x = 0.00, 0.02, 0.04, 0.06, 0.08 and 0.1) by using PUND method. PUND is one of the methods which are used for finding the true value of remnant polarization [41]. The PUND measurements are carried out by the functions of pulse width (PA), pulse amplitude (PA) and pulse delay time (PD). The PUND measurements are standard characterization based on pulses. The PUND measurement techniques can be instigating elsewhere [42]. In the graph 4 pulse width is equal to one unit and similar for time delay. First pulse which is above from normal position is used to measure the total polarization with switching charge density. If switching polarization add with leakage polarization, then it is equal to total polarization ($P^*= P_{switching} + P_{leakage}$). Second pulse tells about total polarization without switching charge density (Q_{sw}). Third and fourth pulse is similar to first and second respectively but in negative bias maximum potential. Along with this the sample showed lower value of leakage current. For finding switching charge density following relation is used Switching charge density (Q_{sw}) is equal to the difference of Switching polarization (P^*) and un-switching polarization ($P^\wedge$) [43]. The difference between P^* and $P^\wedge$ leakage mechanism is back to effect of

switching ferroelectric domain and polarization contribution [44]. In our results at x = 0.02 it shows the minimum leakage current and maximum value of switching charge density 13.8 × 10^{-4}nC/cm^2. Results of these material show ferroelectric properties with the most suitable value of remnant polarization compare with other composition; hence it has potential to be used in energy storage applications.

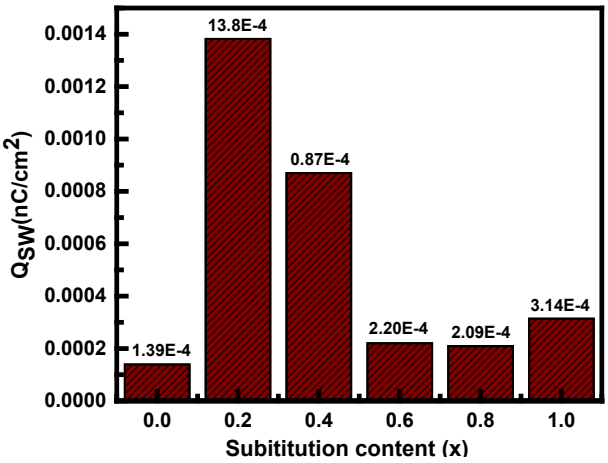

Figure 5. Switching charge density for x = 0.0, 0.02, 0.04, 0.06, 0.08 and 0.1.

From above Figure 5 it is clear that value of switching charge (*P**) is greater than un-switching charge due to remanant polarization. Along with this the sample showed that sample has lower value of leakage current. For finding switching charge density following relation is used:

$$Q_{sw} = P^{*} - P^{\wedge}$$

In Table 2 it is seen that the material has maximum switching density at x= 0.02 which suggest that the sample is ideal at this concentration for storage application

Table 2 Total polarization, polarization without switching and switching charge density of sample.

$PbTi_{1-x}Fe_xO_3$	Total polarization	Polarization without switching	Switching charge density
X=	P^{*} (nC/cm^2)	$P^{\wedge}$ (nC/cm^2)	Q_{sw} (nC/cm^2)
0.00	0.318513	0.318374	0.000139
0.02	0.553111	0.551729	0.001382
0.04	0.193081	0.192994	0.000087
0.06	0.295975	0.295755	0.000220
0.08	0.393291	0.393082	0.000209
0.1	0.431127	0.430813	0.000314

4. Conclusion

The iron-doped titanate ($PbTi_{1-x}$ Fe_xO_3) was successfully synthesized using the sol-gel auto-combustion method with varying iron concentrations (x = 0.00, 0.02, 0.04, 0.06, 0.08, and 0.1). The incorporation of iron at different concentrations was confirmed through EDS analysis. SEM images were used to study the morphology of both un-doped and iron-doped samples. SEM analysis revealed that particle size decreased with increasing doping concentration, from 100 nm to 20 nm.

This suggests that Fe doping influences particle size and agglomeration, which is beneficial for various applications. The ferroelectric properties were analyzed using P-E loops, which showed a decrease in maximum polarization and remanent polarization with higher doping concentrations. However, Fe doping improved the coerctivity. The PUND analysis confirmed the ferroelectric nature, showing minimal leakage current and maximum switching charge density at x = 0.02. This makes Fe-doped $PbTiO_3$ at this concentration ideal for energy storage applications. In summary, Fe-doped $PbTiO_3$ enhances both electrical and structural properties, improving ferroelectric performance and reducing particle size at x = 0.02, suggesting this composition as the optimal choice for practical applications in energy storage, sensors, and memory storage.

Acknowledgement

The authors extend their appreciation to Taif University, Saudi Arabia for supporting this work through project number (TU-DSPP-2024-20).

References

[1] Slimani, Y., Shirsath, S. E., Erdemi, H., Meena, S. S., Batoo, K. M., Almessiere, M. A., Shariq, M. (2024), Ceramics International, 50(13), 22583-22598; https://doi.org/10.1016/j.ceramint.2024.03.360

[2] Slimani, Y., Almessiere, M. A., Shirsath, S. E., Hannachi, E., Baykal, A., Alwadai, N., Ercan, I. (2023), Inorganic Chemistry Communications, 153, 110753; https://doi.org/10.1016/j.inoche.2023.110753

[3] Das, S. K., Mishra, R. N., Roul, B. K. (2014), Solid state communications, 191, 19-24; https://doi.org/10.1016/j.ssc.2014.04.001

[4] Craciun, F., Cordero, F., Cernea, M., Fruth, V., Atkinson, I., Stanica, N., Galassi, C. (2019), Ceramics International, 45(7), 9390-9396; https://doi.org/10.1016/j.ceramint.2018.08.147

[5] Pilch, M., Molak, A. (2014), Journal of alloys and compounds, 586, 488-498; https://doi.org/10.1016/j.jallcom.2013.10.103

[6]Lin, F., Li, Z., Sun, B., Peng, W., Cao, Z., Gao, K., Ren, F. (2024), Materials Today Advances, 22, 100506; https://doi.org/10.1016/j.mtadv.2024.100506

[7]Zheng, T., Deng, H., Zhou, W., Zhai, X., Cao, H., Yu, L., Chu, J. (2016), Ceramics International, 42(5), 6033-6038; https://doi.org/10.1016/j.ceramint.2015.12.157

[8]Nayak, A., Patri, S. K.,Behera, B. (2024), Materials Science and Engineering: B, 309, 117633; https://doi.org/10.1016/j.mseb.2024.117633

[9] Wang, L., Yuan, P., Wang, F., Liang, E., Sun, Q., Guo, Z., Jia, Y. (2014), Materials Research Bulletin, 49, 509-513; https://doi.org/10.1016/j.materresbull.2013.08.075

[10] Gumiel, C., Calatayud, D. G. (2022), Boletín de la Sociedad Española de Cerámica y Vidrio, 61(6), 708-732; https://doi.org/10.1016/j.bsecv.2021.08.002

[11]Varignon, J., Bristowe, N. C., Bousquet, E., Ghosez, P. (2020), Physical Sciences Reviews, 5(2), 20190069; https://doi.org/10.1515/psr-2019-0069

[12]Ramesh, R., Spaldin, N. A. (2007), Nature materials, 6(1), 21-29; https://doi.org/10.1038/nmat1805

[13] Liao, J., Dai, S., Peng, R. C., Yang, J., Zeng, B., Liao, M., Zhou, Y. (2023), Fundamental Research, 3(3), 332-345; https://doi.org/10.1016/j.fmre.2023.02.010

[14] Kumar, M., Shankar, S., Kumar, A., Anshul, A., Jayasimhadri, M., Thakur, O. P. (2020), Journal of Materials Science: Materials in Electronics, 31, 19487-19510; https://doi.org/10.1007/s10854-020-04574-2

[15]Gupta, R., Kotnala, R. K. (2022), Journal of Materials Science, 57(27), 12710-12737; https://doi.org/10.1007/s10853-022-07377-4

[16] Gautam, C., Madheshiya, A. (2020), Journal of Materials Science: Materials in Electronics, 31(15), 12004-12025; https://doi.org/10.1007/s10854-020-03831-8

[17]Xiong, J., Wang, Z., Yang, X., Long, X., He, C. (2021), IEEE Transactions on Ultrasonics, Ferroelectrics, and Frequency Control, 68(8), 2775-2780; https://doi.org/10.1109/TUFFC.2021.3079401

[18] Nougaret, L., Kassa, H. G., Cai, R., Patois, T., Nysten, B., van Breemen, A. J., Jonas, A. M. (2014), ACS nano, 8(4), 3498-3505; https://doi.org/10.1021/nn406503g

[19] Mitra, R., Prusty, A., Manju, U. (2023), Perovskite Metal Oxides (pp. 617-643). Elsevier; https://doi.org/10.1016/B978-0-323-99529-0.00022-9

[20] Guo, J., Chen, W., Chen, H., Zhao, Y., Dong, F., Liu, W., Zhang, Y. (2021), Advanced Optical Materials, 9(23), 2002146; https://doi.org/10.1002/adom.202002146

[21] Shi, P. P., Tang, Y. Y., Li, P. F., Liao, W. Q., Wang, Z. X., Ye, Q.,Xiong, R. G. (2016), Chemical Society Reviews, 45(14), 3811-3827; https://doi.org/10.1039/C5CS00308C

[22] Muhammad, Z., Ishafaq, M. U. U., Zhang, X., Ullah, S., Adam, M. L., Moses, O. A., Zhao, W. (2023) Journal of Alloys and Compounds, 956, 170337; https://doi.org/10.1016/j.jallcom.2023.170337

[23] Ivanov, S. A., Stash, A. I., Riekehr, L., Chen, Y. S., Ye, Z. G. (2020), Scientific Reports, 10(1), 14567; https://doi.org/10.1038/s41598-020-71438-4

[24]Bormanis, K., Kalvane, A., Burkhanov, A. I., Serezhkin, A. M. (2011), Lithuanian Journal of Physics, 51(4); https://doi.org/10.3952/lithjphys.51416

[25] Evans, D. M., Alexe, M., Schilling, A., Kumar, A., Sanchez, D., Ortega, N., Gregg, J. M. (2015), The nature of magnetoelectric coupling in Pb (Zr, Ti) O3Pb (Fe, ta) O3; https://doi.org/10.1002/adma.201501749

[26]Muhammad, Z., Ishafaq, M. U. U., Zhang, X., Ullah, S., Adam, M. L., Moses, O. A., Zhao, W. (2023), Journal of Alloys and Compounds, 956, 170337; https://doi.org/10.1016/j.jallcom.2023.170337

[27]Turjo, R. M. (2014). Structure-property relationship of Ba2+ and Ti4+ doped multiferroic bismuth ferrite.

[28] Ganegoda, H., Mukherjee, S., Ma, B., Olive, D. T., McNeely, J. H., Kaduk, J. A., Segre, C. U. (2021), The Journal of Physical Chemistry C, 125(22), 12342-12354; https://doi.org/10.1021/acs.jpcc.1c02297

[29] Muhammad, Z., Ishafaq, M. U. U., Zhang, X., Ullah, S., Adam, M. L., Moses, O. A., Zhao, W. (2023), Journal of Alloys and Compounds, 956, 170337; https://doi.org/10.1016/j.jallcom.2023.170337

[30]Sakout, Y., El Ghadraoui, O., Lahrar, E. H., Zouhairi, M., Tijani, N., Harrach, A., El Yamni, K. (2024), Journal of Electronic Materials, 53(1), 141-156; https://doi.org/10.1007/s11664-023-10741-y

[31]Nayak, A., Patri, S. K., Behera, B. (2024), Materials Science and Engineering: B, 309, 117633; https://doi.org/10.1016/j.mseb.2024.117633

[32] M. S. Hasan, M. I. Khan, S. Kanwal, M. I. Irfan, Tahani, I. Al-Muhimeed, S. Mumtaz. (2022), Digest Journal of Nanomaterials and Biostructures. 17(4), 1527-1533; https://doi.org/10.15251/DJNB.2022.174.1527

[33] Murtaza, G., Ahmad, R., Rashid, M. S., Hassan, M., Hussnain, A., Khan, M. A., Riaz, S. (2014), Current Applied Physics, 14(2), 176-181; https://doi.org/10.1016/j.cap.2013.11.002

[34] Redhu, P., Punia, R., Hooda, A., Malik, B. P., Sharma, G., & Sharma, P. (2020), Ceramics International, 46(11), 17495-17507; https://doi.org/10.1016/j.ceramint.2020.04.045

[35] Keswani, B. C., Devan, R. S., Kambale, R. C., James, A. R., Manandhar, S., Kolekar, Y. D., & Ramana, C. V. (2017), Journal of Alloys and Compounds, 712, 320-333; https://doi.org/10.1016/j.jallcom.2017.03.301

[36]Nayak, A., Patri, S. K., & Behera, B. (2024), Materials Science and Engineering: B, 309, 117633; https://doi.org/10.1016/j.mseb.2024.117633

[37]Ullah, M. B., Ahamed, J. U., Rubel, R. R., Rahman, M. A., Hasan, Z., Alam, M. K., Khan, M. N. I. (2024), Ceramics International, 50(6), 9604-9616; https://doi.org/10.1016/j.ceramint.2023.12.279

[38] Keswani, B. C., Devan, R. S., Kambale, R. C., James, A. R., Manandhar, S., Kolekar, Y. D., Ramana, C. V. (2017), Journal of Alloys and Compounds, 712, 320-333; https://doi.org/10.1016/j.jallcom.2017.03.301

[39] Sharma, P., Berwal, N., Ahlawat, N., Maan, A. S., Punia, R. (2019), Ceramics International, 45(16), 20368-20378; https://doi.org/10.1016/j.ceramint.2019.07.013

[40] Li, C. X., Yang, B., Zhang, S. T., Zhang, R., Sun, Y., Wang, J. J., Cao, W. W. (2013), Ceramics International, 39(8), 8701-8708; https://doi.org/10.1016/j.ceramint.2013.04.052

[41]Chaudhuri, A. R., Krupanidhi, S. B. (2010), Solid state communications, 150(13-14), 660-662; https://doi.org/10.1016/j.ssc.2009.12.023

[42] http://www.ferrodevices.com/applicationnotes.html

[43] Mahmoud, A. E. R., & Parashar, S. K. S. (2019), Materials Science and Engineering: B, 246, 13-20; https://doi.org/10.1016/j.mseb.2019.05.022

[44]Dawber, M., Rabe, K. M., & Scott, J. F. (2005), Reviews of modern physics, 77(4), 1083-1130; https://doi.org/10.1103/RevModPhys.77.1083